Photo-crosslinked Non-Isocyanate Polyurethane Acrylate (NIPUA) coatings through a transurethane polycondensation approach

Pierre Boisaubert, Nasreddine Kébir, Anne-Sophie Schuller, Fabrice Burel

Photo-crosslinked Non-Isocyanate Polyurethane Acrylate (NIPUA) coatings through a transurethane polycondensation approach.

Pierre Boisaubert[1], Nasreddine Kébir[1],* Anne-Sophie Schuller[2] and Fabrice Burel[1]

[1] Normandie Université, INSA Rouen Normandie, Laboratoire PBS, UMR CNRS 6270 & FR 3038, Avenue de l'Université, 76801 Saint Etienne du Rouvray, France.

[2] Université de Haute-Alsace, Institut Jean Baptiste Donnet, Laboratoire LPIM, EA 4567, 3 bis rue Alfred Werner, 68093 MULHOUSE Cedex France

Correspondence to: Nasreddine KEBIR (E-mail: *nasreddine.kebir@insa-rouen.fr*)

ABSTRACT

A transurethane polycondensation pathway has been used to produce acrylate terminated Non-Isocyanate PolyUrethane (NIPUA) oligomers (A-OI) with controlled molecular weights and chemical structures. These compounds were then photo-crosslinked under UV radiations to afford several NIPU acrylate coatings. The influence of the content in urethane functions as well as the chemical structures on the thermal and mechanical properties of the final coatings has been demonstrated. The obtained coatings exhibited thermal stabilities above 255 °C, Young modulus ranging from 2.6 to 9.2 MPa, tensile strength up to 11.8 MPa and elongation at break varying from 20 to 520 %.

KEYWORDS:

Polyurethane; non-isocyanate; NIPU; transurethanization; coating; acrylates; UV-Curing

INTRODUCTION

Polyurethanes (PUs) are a very important family of polymer materials displaying versatile properties and chemical structures, which afford them a large spectrum of application fields such as shipbuilding, biomaterials, automotive, paints, coatings, adhesives, clothes and footwears.

Polyurethane acrylate systems (PUAs) are formulations containing acrylate-terminated resins that are widely used to produce protective coatings. These coatings generally have very good abrasion resistance, high chemical resistance and very flexible mechanical properties.[1,2] PUAs are conventionally obtained by functionalizing hydroxyl-terminated oligomers, synthesized by the conventional reaction between polyols and toxic diisocyanates, which are synthesized from amines and toxic phosgene.[3] Since the early 2000s, some groups have begun to adapt the synthesis of PUA materials by non-isocyanate routes (NIPUAs).[4-11]

Some works have described the photochemical crosslinking of poly(hydroxyurethane) acrylate (PHUA) oligomers, obtained by polyaddition of cyclic dicarbonate and diamine monomers followed by various functionalization techniques.[8,9,12-14] However, as far as we know, no studies have been carried out on the photo-crosslinking of NIPUA systems obtained by the transurethane polycondensation reaction, which is one of the most promising free isocyanate routes to polyurethanes.[15-21] This technique involves the reaction of dialkyl dicarbamates[15-18] or dihydroxyethyl dicarbamates[19-21] with diols, in presence of organic or organo-metallic catalysts. However, with dihydroxyethyl dicarbamates, a back-biting side reaction may occur at certain conditions leading to formation of urea moieties.[19-21] On the other hand, unlike the aminolysis of cyclic carbonate route leading to poly(hydroxyurethane) structures (PHUs),[22-24] this technique has the advantage of yielding conventional PU structures. Another advantage of this approach, is the wide choice of BMC monomers comparing to diisocyanate monomers, which offers a higher potential for variations in structure and properties of the final polyurethane materials.

In this work, we describe the synthesis of new NIPUA oligomers through the use of the transurethane polycondensation reaction between dialkyl dicarbamates and diols, followed by an acrylation step. The preparation of coatings by photo-crosslinking of the prepared NIPUAs as well as the assessment of their thermal and mechanical properties are reported.

EXPERIMENTAL

Materials

Poly(tetramethylene oxide) (PTMO) of M_n = 650 and 2000 g/mol, 1,6-diaminohexane (98%), 1,5,7-triazabicyclo[4.4.0]dec-5-ene (TBD, 98%), dimethyl carbonate (DMC, 99%, anhydrous), 1,4-butanediol (99%), and 4,4'-methylenebis(cyclohexylamine) (H_{12}MDA, >98%) were obtained from Sigma Aldrich. Acryloyl chloride (96%), trimethylolpropane (TMP, 99%), 4-methoxyphenol (MeHQ, 99%) and triethylamine (99%) were supplied by Fisher Scientific. Diphenyl(2,4,6-trimethylbenzoyl)phosphine oxide (Irgacure 819 or BAPO) and Ethyl phenyl(2,4,6-trimethylbenzoyl) phosphinate (TPO-L or LucirinL) were supplied by BASF. All the other reagents and solvents were used without further purification.

Synthesis

Preparation of dimethyl dicarbamate monomers

In a round-bottomed flask equipped with a magnetic stirrer, diamine (1 eq.), TBD (0.1 eq.) and DMC (10 eq.) were added and stirred for 5 h at 80°C (24 h for BMC-H_{12}). The reaction medium was then cooled to room temperature. Crystallized products (BMC-C_6 and BMC-H_{12}) were recovered by filtration (yield > 85 %) and washed by distilled water to remove TBD. In the case of BMC-Pr, the liquid product was washed with distilled water in diethyl ether medium. Then, the organic phase was dried over $MgSO_4$, filtrated and the solvent was evaporated.

Dimethylhexane-1,6-dicarbamate (BMC-C_6)

^{1}H NMR (300 MHz, $CDCl_3$, δ): 4.67 (s, broad, 2H; N*H*), 3.65 (s, 6H; NH(CO)OC*H*$_3$), 3.15 (m, 4H; NHC*H*$_2$); 1.48 (m, 4H; NHCH$_2$C*H*$_2$), 1.32 (m, 4H; NHCH$_2$CH$_2$C*H*$_2$). **^{13}C NMR** (75 MHz, $CDCl_3$, δ): 26.2, 29.9, 40.7, 52.0, 157.1 ; IR (ATR): ν~3300 cm^{-1} (m; ν_{NH}), ~1700 (s, $\nu_{CO\ H\text{-}bonded}$) cm^{-1}, ~1530 cm^{-1} (s, $\nu_{NH\ bending}$). DSC: T_m=115°C.

4,4'-methylenebis(cyclohexylamine) (BMC-H_{12})

^{1}H-NMR (300 MHz, $CDCl_3$, δ): 3.77 and 3.40 (m, 2H; NHCH); 3.66 (s, 6H; NH(CO)OCH$_3$), 2.1 to 0.75 (20H; methylene and cycle CH and CH$_2$). **^{13}C-NMR** (75 MHz, $CDCl_3$, δ): 156.4 (C=O), 51.9 (OCH$_3$), 50.5 (NHCH), 47.1 (NHCH), 44.1 (NHCHCH$_2$), 42.9 (NHCHCH$_2$), 33.7 and 33.6 (CH), 33.4 (bridge CH$_2$), 32.6 (CH), 32.0 (bridge CH$_2$), 29.7 (CH$_2$), 28.0 (CH$_2$). DSC: T_m= 189 °C.

Dimethyl Dicarbamate of Priamine 1074 (BMC-Pr)

^{1}H-NMR (300 MHz, $CDCl_3$, δ): 4.68 (s, broad, 2H; NH), 3.65 (s, 6H; NH(CO)OCH$_3$), 3.15 (m, 4H; NHCH), 2 to 1 (54H; CH and CH$_2$), 0.87 (m, 6H, CH$_3$). **^{13}C-NMR** (75 MHz, $CDCl_3$, δ): 157.2 (C=O), 52.0 (OCH$_3$), 41.2 (NHCH$_2$), 37.2 (CH$_2$), 33.7 (CH$_2$), 32.0 (CH$_2$), 30.1 (CH$_2$), 29.8 (CH$_2$), 29.6 (CH$_2$), 29.4 (CH$_2$), 26.8 (CH$_2$), 22.8 (CH$_2$), 19.8 (cycle CH), 14.2 (CH$_3$). DSC: T_m<-70 °C.

Preparation of hydroxy-terminated NIPU oligomers (H-OI)

In a three-necked round-bottom flask equipped with a mechanical stirrer, a Dean Stark condenser and connected to a vacuum pump (or a 5 L-four-necked-jacketed glass reactor equipped with a mechanical stirrer and thermometer for 1kg scale), bismethylcarbamate (BMC), poly(tetramethylene oxide) (PTMO) and chain extender were added at an appropriate molar ratio previously calculated by Carothers theory to reach the desired M_n. The temperature was progressively risen to 160 °C under nitrogen flow and stirring. Then, 10 mol% KOMe catalyst relative to BMC monomer was added. After 1 h of reaction at 160 °C, Dean Stark condenser was removed

and the reaction mixture was placed under vacuum (400 mbar, 1 h). Finally, the pressure was carefully reduced to 0.5 mbar for 4 h. After cooling to room temperature under nitrogen flow, the obtained oligomers were recovered without any purification. In the case of using BD as chain extender, evaporation was quantified by NMR calculations. In order to obtain the oligomer with the right molecular weight, the experiment was performed a second time, adjusting BD equivalents.

Preparation of Acrylate-terminated NIPU Oligomers (A-Ol)

In a round bottom flask equipped with a magnetic stirrer (or a 5 L-four-necked-jacketed glass reactor equipped with a mechanical stirrer and thermometer for 1kg scale), a hydroxy-terminated NIPU oligomer was introduced, under a nitrogen stream. The oligomer was solubilized in anhydrous DCM. Triethylamine (3.5 eq.), previously distilled over KOH pellets, was added to the reaction mixture. After cooling the mixture to 0 °C with an ice bath, acryloyl chloride (3 eq.) was added dropwise to the reaction mixture. Then, the mixture was allowed to react for 6 h at room temperature. Filtration of triethylammonium salts was carried out. The mixture was then washed three times by HCl (1M), NaOH (1M) and brine. First organic phase was recovered and the oligomer parts remaining in the aqueous phase were extracted by DCM. The organic phases were combined, dried over $MgSO_4$, and filtrated. 4-methoxyphenol stabilizer was added (from 100 to 500 ppm depending of the oligomer molecular weight) and solvent was evaporated. Finally, the resulting yellow product was dried using high vacuum at 25°C.

Preparation of photo-crosslinked NIPU coatings (NIPUAs)

The formulations were prepared by dissolving A-Ol in an appropriate amount of butyl acetate to reach a convenient viscosity. Subsequently, 3.3 wt% of BAPO-TPOL photoinitiator mixture (1:1) was added to the medium. Formulations were stirred (heated to 70 °C if necessary) for 2 hours to obtain homogeneous medium. Then, the formulations obtained were cast on rigid mat steel "Q-panel" plates supplied by Labomat. After degreasing the plates with a cloth soaked in ethanol (EtOH), two types of coatings were obtained for each type of formulation, i.e “thin” and “thick” films. In order to obtain thin films, the desired formulation was applied on top of the plate and the wet thickness was controlled by a roll coater. To obtain thick films, blades of adhesive tape were used on the edges to calibrate the thickness. The plates were then placed in a UV conveyor (UV Fusion Light Hammer 6) to perform the photo-crosslinking.

Measurements and Instrumentation

^{1}H and ^{13}C NMR analysis were performed on a Bruker 300 Fourier Transform spectrometer at 300 MHz and 75 MHz, respectively, in $CDCl_3$ solutions containing tetramethylsilane (TMS) as internal standard. FTIR spectra were acquired with Perkin-Elmer Spectrum 2000 FTIR, provided with a diamond ATR device (Attenuated Total Reflection). Spectra were recorded from 10 scans in the 650 to 4000 cm^{-1} range.

Average molecular weights of polymers (M_n and M_w) and dispersity (Đ = M_w/M_n) were assessed by Size Exclusion Chromatography (SEC). Polymers were dissolved in dichloromethane, filtered (0.45 µm) and analyzed at 25°C by a Varian PL-GPC50 system provided with two mixed packed columns (PL gel mixed type C). Dichloromethane was used as the mobile phase and PMMA standards (from 875 to 62000 g mol^{-1}) were used for calibration.

Thermo-Gravimetric Analysis (TGA) was achieved with a TGA Q500 device (TA Instruments), using a heating rate of 10°C/min under a nitrogen flow. The temperature at 5% of weight loss ($T_{5\%}$) was used as reference to estimate the degradation of polymers.

Differential Scanning Calorimetry (DSC) analysis was performed with a DSC Q2000 device (TA Instruments), using a heating rate of 10°C/min under a nitrogen flow. The midpoint method was used to evaluate the glass transition temperature (Tg). Melting temperature (T_m) was measured at the maximum of the endothermic signal. DSC curves were recorded in a temperature range of -70 to 250°C.

The thickness of crosslinked thin films was measured in accordance with ISO 2808: 2007 by magnetic determination using the PosiTector 6000. Films characterized by this device had thicknesses of less than 50 µm with an accuracy of ± 1.0 micron. The device consists of a probe to be applied against the coating, previously deposited on a flat surface. The thickness of the thick crosslinked films (between 100 µm and 1 mm) was measured with the Digimatic micrometer, with an accuracy of ± 1.0 micron. The coating was clamped by a micrometer screw between the two circular measuring surfaces of the device.

The tensile analyses were performed on a Zwick/Roell device equipped with a 500 N force sensor, two jaws (pneumatic or manual clamping, depending on the type of sample characterized) and a movable crosshead. The tests were carried out in accordance with ISO 527_3 "Test conditions for films and foils". For each coating, between 5 and 15 rectangular specimens were cut out with a scalpel. Specimens with unevenness or notches were systematically removed. The manually clamped jaws limit the width of the specimens to 6 mm, the specimens had the following dimensions: a total length l_3 of 50 mm; a width b of exactly 4 mm; a thickness h always less than 1 mm. The values of b and h were measured precisely at three points and the average of the three measurements were used for the calculations. The distance between jaws L_0 is fixed at 35 millimetres. The test speed υ was fixed at 20 mm/min, and the preload value was maintained at 0.05 MPa. After each sample has been broken, the following values shall be determined as a function of the cross-section A (A = b × h, expressed in mm^2) of the sample: The breaking strength of the material σ_r (MPa) which corresponds to the stress experienced when the specimen breaks, equal to the maximum stress; the elongation at break ε_r (%) which corresponds to the elongation of the material before it breaks; Young's modulus or Elasticity E (MPa) which corresponds to the slope of the stress/strain curve in the range between ε_1 = 0.05% and ε_2 = 0.25% of the elongation of the material considered reversible.

For swelling tests, mass (mi) samples of approximately 15 mg (thin films) and 50 mg (thick films) are placed in 4 mL pill dispensers containing 3.5 mL volume of THF and then placed under magnetic agitation at room temperature for 24 hrs. The samples were removed from the solvent, dried on the surface with absorbent paper and weighed (m_h). These samples were then dried in a vacuum oven at 40°C for 24 h and weighed (m_f). Then, we have calculated:

- The extractables rate (τ_{EX}) of the samples, expressed in %:

$$\tau_{EX} = \frac{m_i - m_f}{m_i} \times 100 \qquad \text{Eq.1}$$

- The swelling (Q) of the samples, expressed in %:

$$Q = \frac{m_h - m_f}{m_f} \times 100 \qquad \text{Eq.2}$$

RESULTS AND DISCUSSION

Synthesis and characterizations of acrylated NIPUs oligomers

Bis(methyl carbamate) monomers (BMC, Scheme 1) were prepared by reacting a large excess of dimethylcarbonate (DMC) (to avoid cyclization and chain extension) with several diamines, using TBD as catalyst, as previously described.[16-18] The monomers mixture was allowed to react during 6 h at 80 °C. Three diamines were used, i.e. hexamethylene diamine (C_6) which can be considered as potentially biobased;[25-26] 4,4'-methylenebis(cyclohexylamine) (H_{12}) which is a petroleum-based monomer ; and Priamine (Pr) from Croda which is fully biosourced (from vegetable oils). Furthermore, DMC[27-28] can also be obtained from renewable feedstock. Solid BMCs (C_6 and H_{12}) were recovered by crystallization, whereas liquid BMC-Pr was recovered by extraction in diethyl ether after washing with water.

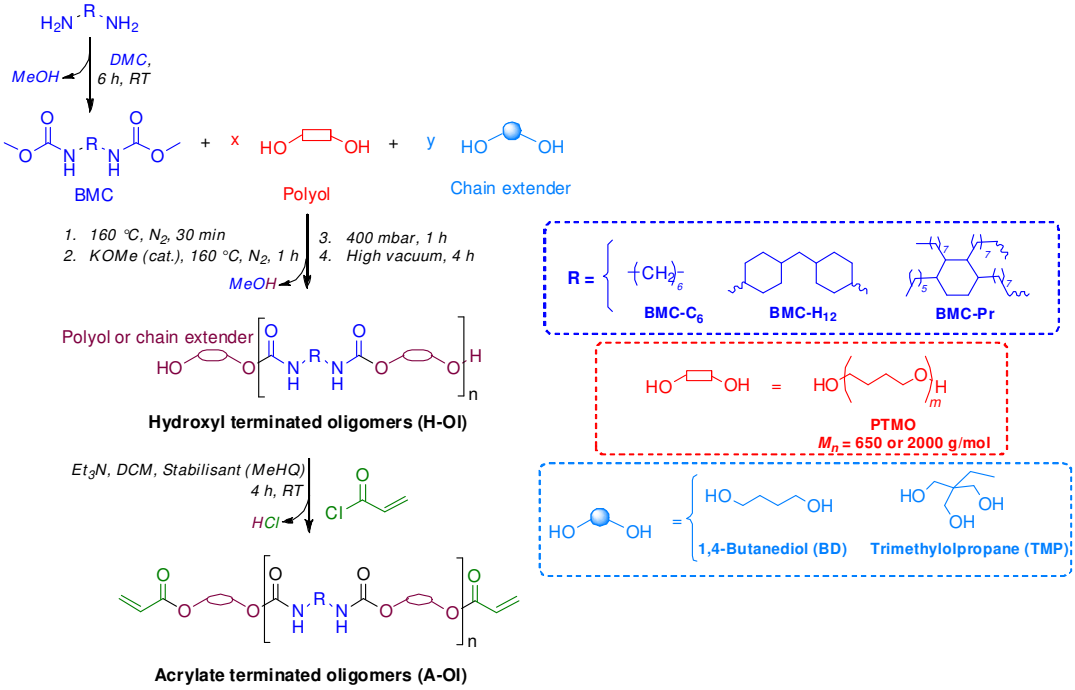

Scheme 1. Synthesis approach of acrylated NIPU oligomers.

In order to obtain NIPU oligomers with hydroxyl chain-ends (H-Ol), the synthesized BMCs were engaged in a transurethane polycondensation reaction with an excess of poly(tetramethylene oxide) (PTMO), a di-hydroxylated polyether with different molecular weights (M_n = 650 or 2000 g/mol) (Scheme 1). PTMO affords interesting properties by giving the final material good resistance to hydrolysis and good mechanical characteristics.[29] The obtained oligomers were denoted "H-BMC-M_nPTMO". As an example, the H-Ol oligomer synthesized from BMC-Pr and PTMO of M_n = 2000 g/mol was denoted "H-Pr-2000". Two NIPU materials bearing butane diol (BD) or trimethylolpropane (TMP) as chain extenders were also prepared (A-C_6-2000/BD-1/2 and A-C_6-650/TMP-1/0.5, respectively).

The targeted M_n values for NIPU series based on PTMO650 and PTMO2000, were of 2000 and 5500 g/mol, respectively. Thus, the targeted X_n was deduced from the following equation:

$$M_n = (X_n - 1) \times M_0 + M_{diol} \quad \text{Eq.3}$$

With:

- M_0 = Molecular weight of the repeating unit = $(M_{diol} + M_{BMC} - 2M_{MeOH})/2$
- M_{diol} = Average molecular weight of "PTMO + chain extender" mixture, with respect to their equivalent ratio.
- M_{BMC} = Molecular weight of BMC.
- M_{MeOH} = Molecular weight of methanol.

Using Carothers' theory,[30] the degree of polymerization "X_n" as well as the number of repeating units "n", can be expressed as follows: [31]

$$X_n = \frac{1 + r}{1 + r - 2rp} = 2n + 1 \quad \text{Eq.4}$$

With:

- r = stoichiometric ratio of reagents, with r < 1
- p = conversion of the limiting reagent monomer.

Assuming that p → 1, the stoichiometric excess of diols to be used « $1/r$ » can be deducted as follows:

$$\frac{1}{r} = \frac{X_n + 1}{X_n - 1} \quad \text{Eq.5}$$

The hydroxy-terminated (H-OI) NIPU oligomers were functionalized by the use of acryloyl chloride to obtain oligomers with acrylate chain-ends designated as A-OI. After reaction at room temperature in DCM, the medium was washed several times with acidic and basic aqueous solutions to remove reaction by-products, and then the A-OI was obtained after drying over $MgSO_4$ and evaporation of DCM. The double bonds were stabilized before the evaporation step by adding around 300 ppm of methoxyphenol (MeHQ) to prevent crosslinking of the products. The A-OI obtained were named "A-BMC-M*n*PTMO".

The FTIR spectra (Figure 1) showed the disappearance of the stretching band of the terminal hydroxyl functions (H-O) at around 3500 cm^{-1}, as well as the appearance of the bending bands of the C-H bond of the acrylate group at around 1410 cm^{-1} (in-plane) and at around 810 cm^{-1} (out-of-plane). The C=O stretching vibration band of the ester-acrylate groups appeared at around 1725 cm^{-1}, and was overlapped with the C=O stretching vibration band of the free urethane groups (1720 cm^{-1}). Other urethane bands were also observed at 1686 cm^{-1} (H-bonded C=O, stretching) and 1526 cm^{-1} (N-H bending). The band at around 3300 cm^{-1} arose from stretching vibration of N-H bonds of urethane groups.

1H NMR analysis (Figure 2) showed that the signal "6" of the terminal methylene groups was strongly shifted by the electron-withdrawal inductive effect of the introduced acrylate groups. (t, from δ = 3.61 ppm (CH_2-OH) to approximately δ = 4.17 ppm (CH_2-OCOCH=CH_2)). The new acrylate proton signals appeared at around δ = 6.39 ppm (signal "10", dd, R-OCOCHCH$_{trans}$H, $^3J_{trans}$ = 17 Hz, 2J ≈ 1 Hz), δ = 6.11 ppm (signal "9", dd, R-OCOCHCH_2, $^3J_{trans}$ = 17 Hz, $^3J_{cis}$ = 10 Hz) and δ = 5.81 ppm

(signal "11", dd, R-OCOCHCH$_{cis}$H, $^{3}J_{cis}$ = 10 Hz, 2J ≈ 1 Hz). 13C NMR analysis (supporting data) revealed the signals of the two acrylate carbons (δ = 130.5 and 128.6 ppm), as well as the quaternary carbon of the acrylate ester group (δ = 166.3 ppm).

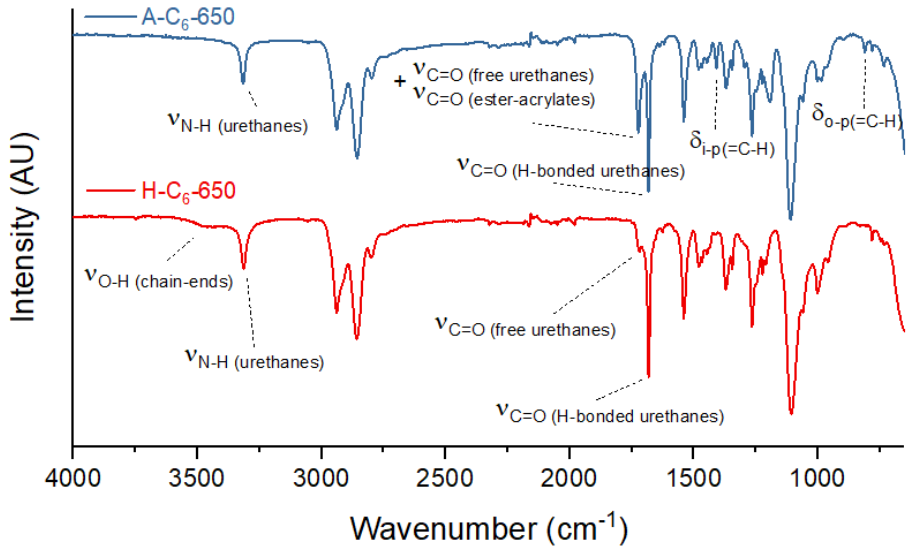

Figure 1: FTIR spectra of the oligomers H-C6-650 and A-C6-650.

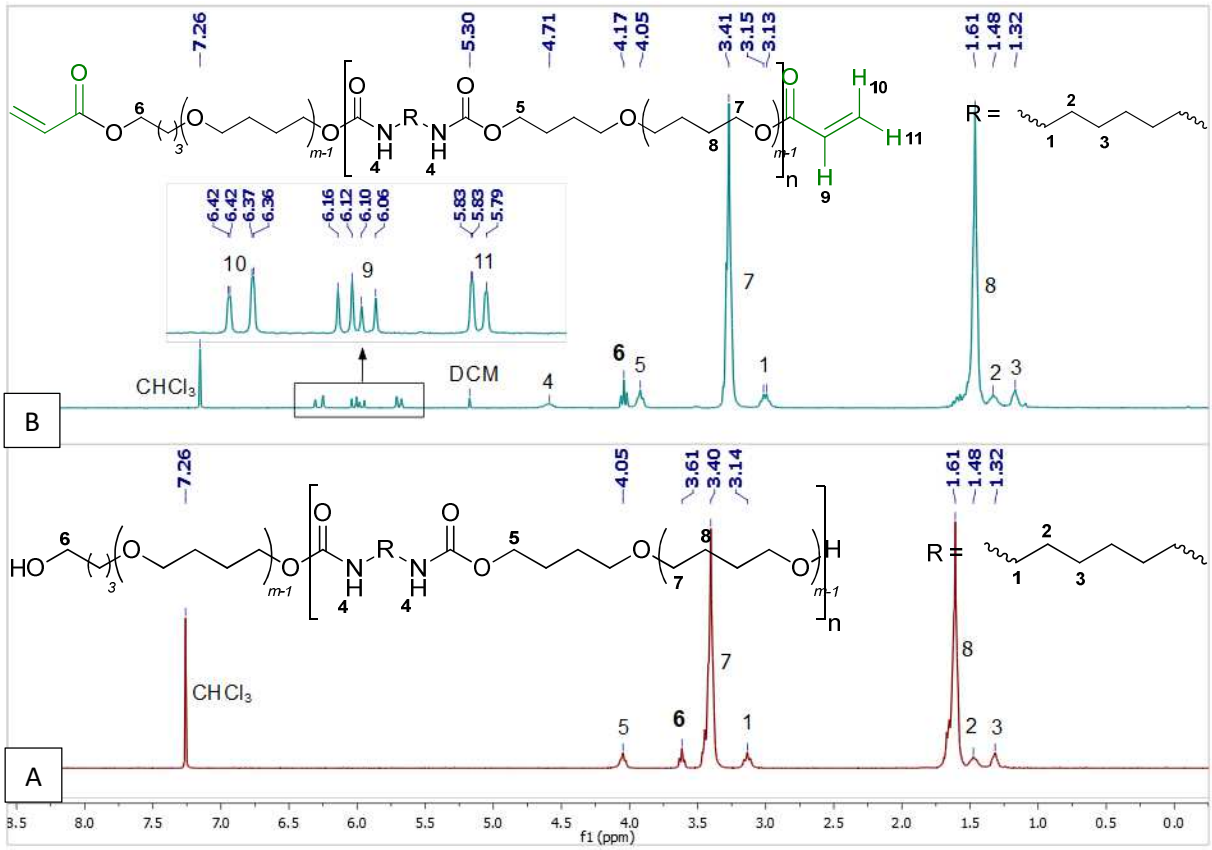

Figure 2: ^{1}H NMR spectra of H-C$_6$-650 (A) and A-C$_6$-650 oligomers (B).

The physico-chemical characteristics of A-Ol are listed in Table 1. They have a yellowish appearance and were obtained in good yields. The lowest yields (59 - 65 %) were obtained with A-C6-

650/TMP-1/0.5 and A-C6-2000/BD-1/2 because of their lower solubility in DCM, which was the reaction and extraction solvent. This low solubility is ascribed to higher percentages of urethane functions and hard segments (%$U_{A\text{-}Ol}$, %HS) within these materials.

Table 1: Physico-chemical characteristics of some prepared A-Ol oligomers.

A-Ol[1]	Step η[2] (%)	Global η[2] (%)	M_n[3] (g/mol)	M_n[4] (g/mol)	Đ[4]	$\%U_{A\text{-}Ol}$ (%HS)[5]	Aspect
A-C_6-650	70	67	1900	2600	2.7	8.7 (12.4)	Waxy and crumbly solids
A-C_6-650-kg	74	68	1750	2750	2.7	8.2 (11.6)	
A-C_6-650-*5030*	87	83	5030	8500	2.7	12.2 (17.5)	
A-C_6-650/TMP-1/0.5	65	59	1750	PS*	PS*	12.1 (21.7)	Soft solid
A-H_{12}-650-kg	88	78	2100	3300	2.4	8.3 (18.2)	Soft solid
A-Pr-650-kg	77	75	1850	1550	5.6	5.7 (28.0)	Oily
A-C_6-2000	75	71	5550	12850	2.0	3.3 (4.9)	Waxy solid
A-C_6-2000-kg	76	72	5650	11100	2.2	3.4 (5.0)	
A-C_6-2000/BD-1/2	59	55	2800	PS*	PS*	9.4 (18.4)	Crumbly solids
A-H_{12}-2000	93	83	5600	11100	2.5	3.2 (7.3)	Viscous oil
A-Pr-2000	96	92	5800	11900	2.2	2.9 (14.6)	Viscous oil

[1] Kg means kilogram scale; the ratio PTMO650/TPM was 1/0.5; the ration PTMO/BD was 1/2)

[2] Step η: Mass yield of Acrylation step; Global η: overall mass yield of the 3 synthesis steps (Scheme 1).

[3] Calculated by ^{1}H NMR.

[4] Calculated by GPC.

[5] Percentage of urethane: $\%U_{A-Ol} = [(2 \times n \times M_{Urethane})/ M_n] \times 100$

Percentage of hard segments:

$\%\mathrm{HS} = [[(a \times (M_{BMC} - 2 \times M_{MeOH}) + b \times (M_{BMC} + M_{Extender} - 2 \times M_{MeOH})) \times n] / M_n \, exp] \times 100$

a = PTMO molar fraction; b = chain extender molar fraction, with " $a + b = 1$".

* Partially soluble in DCM.

In summary, we have obtained more than ten oligomers with exclusively acrylate (A-Ol) chain-ends, using a simple process. The synthesis of some A-Ol was developed on a kilogram scale in a 5-litre reactor, with good mass yields (see Table 1, orange lines). At both laboratory and kilogram scale, the yields obtained throughout the synthesis process were highly dependent on the yields of the acrylation stage (η_{global} = 59 - 92 %).

Preparation and characterizations of photo-crosslinked coatings

The acrylate oligomers A-Ol were formulated with a combination of two type I free-radical photoinitiators (TPO-L and BAPO (1:1), Scheme 2) at 3.3 wt.%, in butyl acetate (AcOBu). The formulations were photo-crosslinked under a UV conveyor equipped with a parabolic mercury vapor lamp. For reproducibility, the light dose received by the sample after one pass was adjusted to about 1.2 J/cm^2 at a total intensity of about 10 W/cm^2 in the UVA + UVB + UVC ranges, the conveyor speed was kept constant at 5 m/min. The coatings were prepared in two sets of thicknesses, i.e. around 50

µm (thin films) and around 200 µm (thick films). The photochemical process was chosen because of its multiple advantages comparing to a conventional thermal process (time and energy savings, etc.).

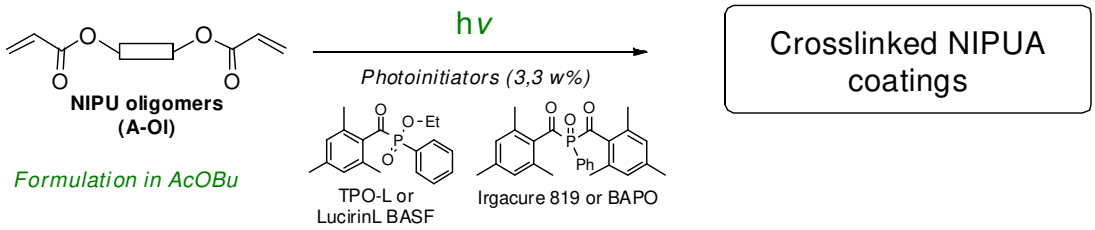

Scheme 2. Photo-crosslinking approach of the A-OI oligomers.

The obtained coatings were yellowish, transparent, smooth and have regular surfaces. Photographs of some obtained coatings are available in the supporting data. However, A-C_6-2000/BD-1/2 was rough and opaque, due to the partial solubilization of the segregated hard segments of this oligomer in AcOBu.

The conversions were calculated by FTIR by monitoring the evolution of the absorbance ascribed to the C-H bond deformation band in the plane of the C=C acrylate group at σ = 1410 cm^{-1}. The conversion χ was calculated as follows:

$$\chi = \frac{\frac{A_0^{C=C}}{A_0^{ref}} - \frac{A_f^{C=C}}{A_f^{ref}}}{\frac{A_0^{C=C}}{A_0^{ref}}} \times 100 \qquad \text{Eq.6}$$

With $A_0^{C=C}$ and $A_f^{C=C}$ the absorbance values of the δ(=C-H) band at 1410 cm^{-1}, of the starting A-OI and the NIPUAs films formed after crosslinking, respectively. A_0^{ref} and A_f^{ref} are the absorbance values of the stretching band of the C-H sp3 bonds of these compounds.

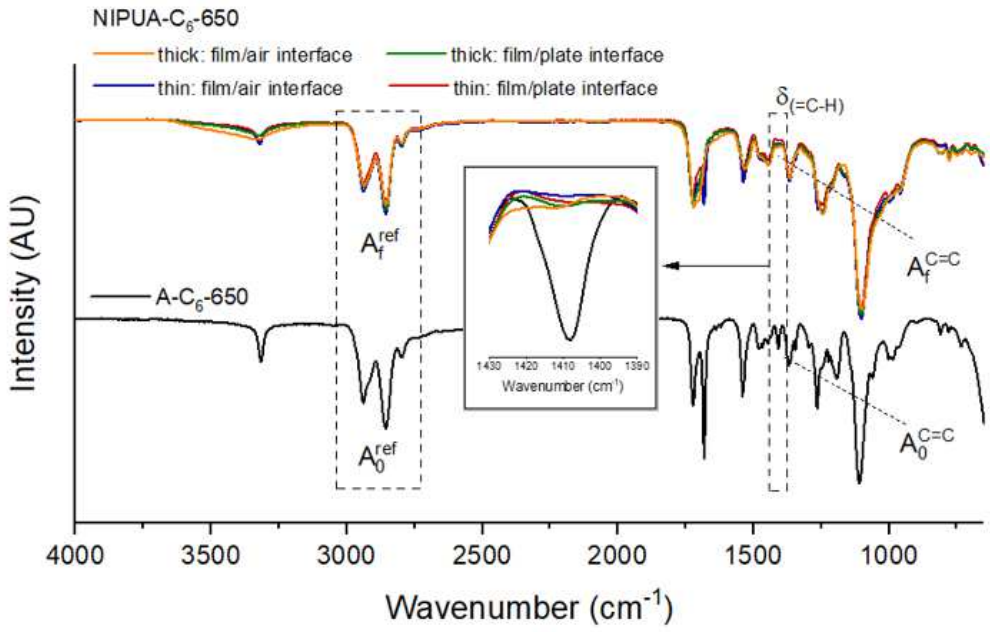

Figure 3. FTIR spectra of several interfaces of thin and thick films NIPUA-C_6-650 before and after crosslinking.

For the NIPUA-C_6-650 film, FTIR spectra were recorded for each side of the thin and thick coatings. The overlay of the bands at 1410 cm^{-1} is shown in Figure 3. No significant differences in conversion were noted at any interface or coating thickness. The study of other films confirmed these claims. Thus, we chose to calculate FTIR conversion only at the film/air interface of thin coatings.

The conversion values (χ) of the acrilic functions are depicted in Table 2. Overall, one can observe that χ values are dependent on the molecular weight of A-Ol. Indeed, A-Ol with molecular weight around 2000 g/mol ($C_{c=c}$ > 2.0 meq/g) exhibited high conversion (χ > 90 %), whereas A-Ol with molecular weight around 5000 g/mol ($C_{c=c}$ > 0.7 meq/g) exhibited lower conversion (χ ≈ 75 %). These conversions are in good agreement with the values in the literature for conventional PUAs systems.[1,2,32]

Table 2: Conversion and appearance of NIPUA coatings.

Coating code	$C_{C=C}$[1] (meq/g)	DE[2] (%)	χ[3] (%)	Aspect[4]	Thickness (μm)
NIPUA-C_6-650	2.4	45	> 95	Y, S, T	24 ± 8 **194 ± 4**
NIPUA-C_6-650-kg	2.6	53	> 95	Y, S, T	23 ± 4 **153 ± 13**
NIPUA-H_{12}-650-kg	2.1	68	90	Y, S, T	28 ± 4 **219 ± 1**
NIPUA-Pr-650-kg	2.4	83	> 95	Y, S, T	40 ± 3 **132 ± 24**
NIPUA-C_6-650/TMP-1/0.5	3.0*	40	> 95	Y, SR, T	10 ± 3 **131 ± 4**
NIPUA-C_6-650-*5030*	0.9	26	84	Y, SR, T	24 ± 4 **153 ± 6**
NIPUA-C_6-2000-kg	0.8	52	75	Y, S, T	28 ± 4 **160 ± 11**
NIPUA-H_{12}-2000	0.8	62	73	Y, S, F, T	23 ± 3 **165 ± 6**
NIPUA-Pr-2000	0.8	61	76	Y, S, F, T	27 ± 5 **205 ± 5**
NIPUA-C_6-2000/BD-1/2	1.6	40	84	Y, SR, O	23 ± 4 **153 ± 9**

[1] Double bond concentration of A-Ol oligomers.

[2] Dry extract from A-Ol AcOBu formulations.

[3] Conversion of acrylate double bonds estimated by FTIR.

[4] Y = Yellow, S = Soft, SR = Semi-rigid, F = Fragile, T = Transparent, O = Opaque.

* Estimated in relation to the theoretical functionality of the A-C6-650/TMP-1/0.5 oligomer (f = 2.33).

In order to discuss the crosslinking properties of the prepared films, we have defined $M_{c(A-A)}$ as the average molecular weight between acrylate functions, i.e. knots of the crosslinked network. With the use of polyfunctional trimethylolpropane (f = 3), $M_{c(A-A)}$ was estimated with respect to the theoretical functionality of the precursor A-C6-650/TMP-1/0.5 (f = 2,33), according to the following equation:

$$M_{c(A-A)} = 2 \times \frac{M_{n(A-Ol)}}{f_{(A-Ol)}} \qquad \text{Eq.7}$$

with $M_{n(A-Ol)}$ and $f_{(A-Ol)}$: the molecular weight and functionality of the A-C6-650/TMP-1/0.5 oligomer, respectively.

The swelling tests were conducted in THF, the percentages of extractables (τ_{Ex}) and swelling (Q) are listed in Table 3. One can observe that the τ_{Ex} values of the NIPUA coatings are below 13 %, and most of them are below 6 %, which is a characteristic of good crosslinked networks. Furthermore, these coatings did not undergo any significant degradation in THF. As expected, crosslinking density, which increases with decreasing $M_{c(A-A)}$, had a clear impact on the swelling properties. Indeed, the swelling percentages of coatings with $M_{c(A-A)}$ values around 2000 g/mol were lower than those of coatings with $M_{c(A-A)}$ values around 5000 g/mol. Nevertheless, thick films, except NIPUA-C_6-2000/BD-1/2 film, swell more in THF than their thin analogues with more and less the same amount of extractables. This complex phenomenon could be ascribed to samples geometric reasons. For $M_{c(A-A)}$ values around 2000 g/mol, swelling percentages ranged from 24 to 45 % for thin films, and from 61 to 121% for thick films. For $M_{c(A-A)}$ values around 5000 g/mol, swelling percentages varied from 127 to 232 % for thin films, and from 287 to 557 % for thick films. Thick NIPUA-C_6-2000/BD-1/2 film, which has $M_{c(A-A)}$ = 2800 g/mol, exhibited and intermediate swelling percentage (266%). However, its thin analogue was out of the trend (Q=f($M_{c(A-A)}$) curves in the supporting data) and displayed a relatively high swelling percentage (281%).

Table 3: Extractables and swelling percentages of NIPUA coatings.

Coating code	$M_{c(A-A)}$ (g/mol) [1]	Thin films		Thick films	
		τ_{Ex} (%)	Q (%)	τ_{Ex} (%)	Q (%)
NIPUA-C_6-650	1900	1.2 ± 0.9	27 ± 2	5.3 ± 0.5	121 ± 3
NIPUA-C_6-650-kg	1750	2.7 ± 0.6	24 ± 0	0.9 ± 0.4	126 ± 4
NIPUA-H_{12}-650-kg	2100	2.2 ± 0.1	34 ± 4	0.9 ± 0.1	95 ± 6
NIPUA-Pr-650-kg	1850	10.4 ± 0.8	45 ± 4	1.0 ± 0.1	61 ± 1
NIPUA-C_6-650/TMP-1/0.5	1500	0.5 ± 0.4	24 ± 2	8.0 ± 0.1	88 ± 12
NIPUA-C_6-650-*5030*	5030	6.6 ± 0.3	136 ± 8	12.8 ± 0.9	557 ± 19
NIPUA-C_6-2000/BD-1/2	2800	6.5 ± 1.7	281 ± 12	4.0 ± 0.3	266 ± 6
NIPUA-C_6-2000-kg	5650	2.4 ± 0.4	180 ± 27	5.3 ± 1.1	313 ± 14
NIPUA-H_{12}-2000	5600	0.6 ± 0.4	232 ± 27	2.8 ± 0.1	287 ± 25
NIPUA-Pr-2000	5800	3.4 ± 0.8	127 ± 2	3.3 ± 1.4	346 ± 62

[1] Average molecular weight between two acrylate functions.

Thermal properties

The thermal stability of the synthesized NIPUA coatings was evaluated by TGA under nitrogen atmosphere. The temperatures at 5% of weight loss ($T_{5\%}$) are displayed in Table 4. Typical TGA curves are shown in Figures 4 and 5. As with conventional polyurethane, [3,33] thermal degradation of NIPUA-OI coatings is a two-step process, with degradation of the hard segment parts (HS, $T_{max} \approx 320$ °C) followed by the PTMO soft segment parts (SS, $T_{max} \approx 410$ °C). $T_{5\%}$ ranged from 255 to 338 °C showing very good thermal stabilities. The A-OI oligomers showed similar two-step degradation profiles, suggesting that crosslinking reaction has no significant influence on thermal stability. TGA curves showed also that NIPUA-650 series are less thermally stable in terms of weight loss than their NIPUA-2000 analogues, which is consistent with a higher concentration of urethane functions within the NIPUA-650 series.

Table 4: Thermal properties of NIPUA coatings.

Coating code	$T_{5\%}$[1] (°C)	T_c[2] (°C)	ΔH_c[2] ($J.g^{-1}$)	T_m[2] (°C)	ΔH_m[2] ($J.g^{-1}$)	$T_\#$[3] (°C)	$\Delta H_\#$[3] (J/g)	T_g[2] (°C)
NIPUA-C_6-650	282	-	-	-	-	139	69	-
NIPUA-C_6-650-kg	304	-	-	-	-	164	7	-
NIPUA-H_{12}-650-kg	290	-	-	-	-	191	13	-45
NIPUA-Pr-650-kg	325	-	-	-	-	168	12	-59
NIPUA-C_6-650/TMP-1/0,5	261	-	-	-	-	158	32	-57
NIPUA-C_6-650-*5030*	296	3	17	34	21	149	18	-
NIPUA-C_6-2000-kg	318	-21	46	13	47	187	17	-
NIPUA- H_{12}-2000	301	-28*	26*	8	26	-	-	-
NIPUA-Pr-2000	338	-37*	32*	9	32	184	18	-
NIPUA-C_6-2000/BD-1/2	285	-30 NV**	28 NV**	11 186**	32 5**	182	21	-

[1] Determined by TGA.

[2] Determined by DSC. Tc: crystallization temperature (1st cooling cycle); Tm: melting temperature (1st heating cycle).

[3] Exothermic phenomena ($T_\#$) determined by DSC from the 1st heating cycle.

* Cold crystallization (1st heating cycle)

** NV = Not visible. Crystallization/melting temperatures of the hard segments.

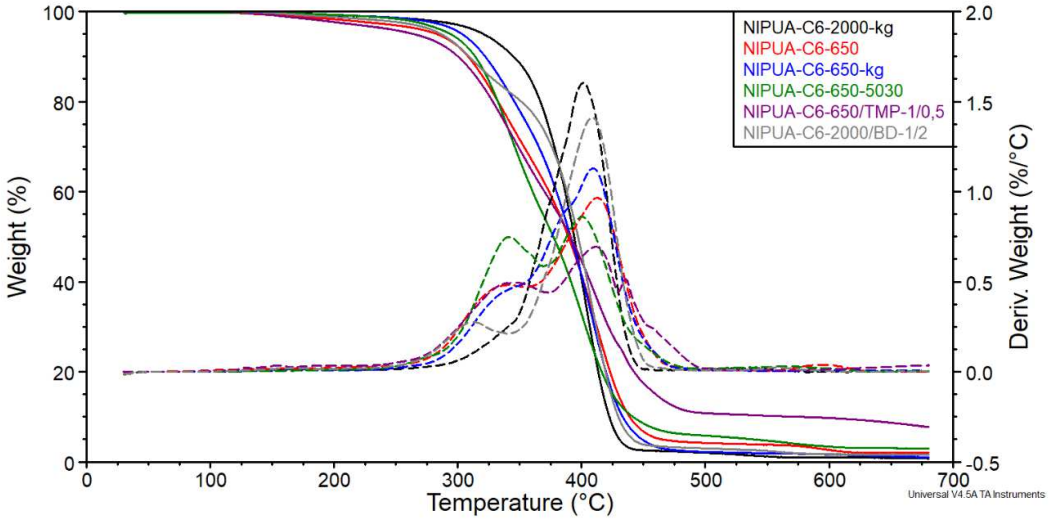

Figure 4: TGA curves (solid) and their first derivative curves (dashed) of NIPUA coatings based on BMC-C_6.

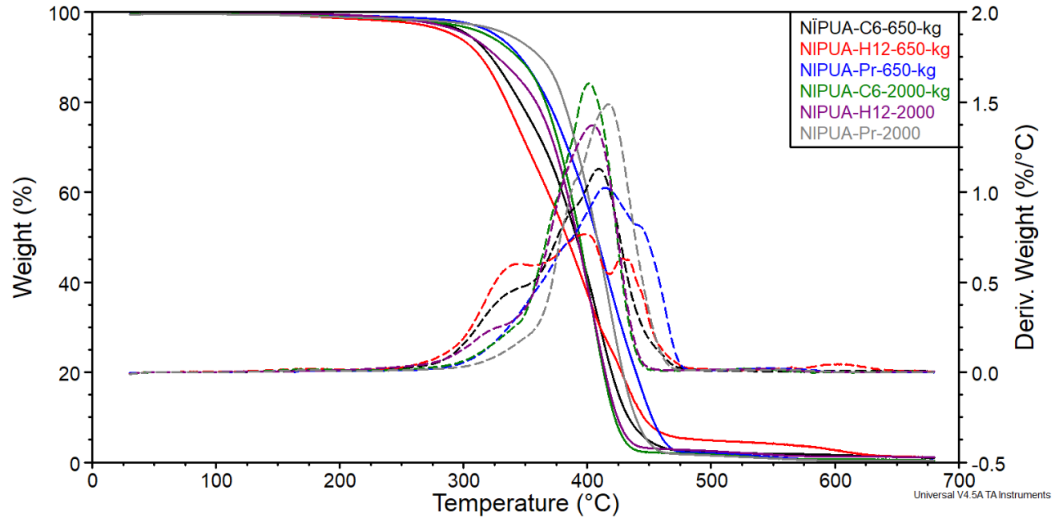

Figure 5: TGA curves (solid) and their first derivative curves (dashed) of NIPUA-OI coatings using different BMC and PTMO types.

The thermal properties of the NIPUA coatings were assessed by DSC. The thermal parameters are presented in Table 4. Typical DSC curves are displayed in Figure 6 and supporting data. The glass transition temperature of the soft segments (Tg (SS)) was observed for only three coatings in the scanned temperature range (T > -60°C). These are NIPUA-H_{12}-650-kg and NIPUA-Pr-650-kg, made with asymmetrical BMC-H_{12} and BMC-Pr respectively, and NIPUA-C_6-650/TMP-1/0.5 containing trimethylolpropane (TMP) as branching agent. These non-regular structures, bearing low molecular weight PTMO650, would promote SS and HS phase interactions and miscibility, which would increase values of Tg (SS).[34] Tg (SS) of the other coatings were not observed in the same scanning conditions, likely due to the higher molecular weight of PTMO2000, their lower urethane content, and the use of symmetrical BMC-C_6 promoting HS - HS interactions.[35] Thus, the Tg values of these materials were probably lower than -70°C, which is the limit of detection of the DSC system used.

It can also be noted that NIPUA coatings with $M_{c(A-A)}$ higher than 2000 g/mol exhibited semi-crystalline behavior. The melting (T_m) and crystallization temperatures (T_c) ranging from 9 to 34°C

and from -37 to 3°C, with associated enthalpy values of 21 to 47 $J.g^{-1}$, and of 17 to 46 $J.g^{-1}$, respectively, correspond to the organized parts of the PTMO soft segments. The melting temperature of the hard segments (T_m= 186°C) was observed only in the case of NIPUA-C_6-2000/BD-1/2, i.e. where a chain extender (BD) is used, but with a low melting enthalpy (5 $J.g^{-1}$) and without any recrystallization during the cooling cycle. This result is often observed in the case of conventional polyurethanes and is due to the low content of hard segments in these materials. Furthermore, an exothermic phenomenon was observed during the first heating cycle of the DSC analysis, which can be explained by the thermal conversion of the residual acrylate groups and/or the degradation of the photoinitiators.

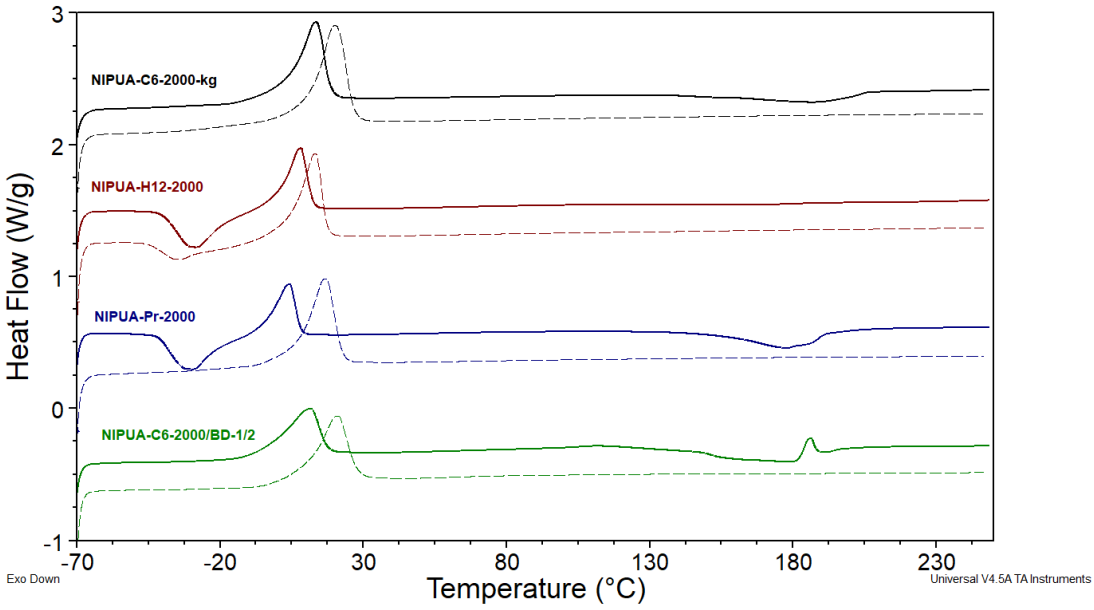

Figure 6: DSC thermograms of NIPUA-2000 film series. 1st heating (solid curves) et 2nd heating (dashed curves).

Mechanical properties

The mechanical properties of the prepared thick NIPUAs films have been studied by the uniaxial tensile test. The results are depicted in Table 5. Typical stress/strain curves are presented in Figures 7 to 10.

For PTMO650-based coatings, the stress/strain curves are shown in Figure 7. The Young's modulus values of these NIPUA series show no significant dependence on the type of BMC used (E between 4.94 and 6.63 MPa, Table 5). These coatings exhibited a low elasticity, with ε_r ranging from 20 to 47%, as well as a low mechanical stress at break (σ_r between 1 and 2 MPa, Table 5).

The stress/strain curves of PTMO2000-based coatings are shown in Figure 8. Comparing to NIPUA-650 series, NIPUA-2000 coatings exhibited lower Young's modulus (E = 2 - 4 MPa) and higher elongations at break (ε_r from 170 to 470 %, Table 5). The breaking stress σ_r ranged from 1.66 to 11.8 MPa. NIPUA based on BMC-C_6 was the most elastic and the most resistant material, which can be explained by its symmetric structure leading to more HS-HS interactions. Furthermore, the shape of its tensile curve implies strain-induced crystallization and self-strengthen.

Table 5: Mechanical properties of NIPUA coatings.

Coating	$M_{c(A\text{-}A)}$[1] (g/mol)	E[2] (MPa)	σ_r[2] (MPa)	ε_r[2] (%)	%HS[3] (%)	$C_{C=C}$[4] (meq/g)
NIPUA-C_6-650-kg	1750	6.63 ± 0.90	1.15 ± 0.24	20 ± 5	12	2.6
NIPUA-C_6-650	1900	4,94 ± 0,39	0,96 ± 0,09	26 ± 5	8,7	2,37
NIPUA-H_{12}-650-kg	2100	6.34 ± 0.51	2.03 ± 0.05	47 ± 2	18	2.1
NIPUA-Pr-650-kg	1850	6.32*	1.32*	29*	28	2.4
NIPUA-C_6-2000-kg	5650	2.69 ± 0.32	11.8 ± 3.5	470 ± 37	4.9	0.8
NIPUA-H_{12}-2000	5600	2.62 ± 0.39	1.66 ± 0.70	210 ± 99	7.3	0.8
NIPUA-Pr-2000	5800	2.60 ± 0.91	1.78 ± 1.28	170 ± 110	14.4	0.8
NIPUA-C_6-650/TMP-1/0,5	1500	7,38 ± 0,77	2,39 ± 0,38	41 ± 8	22	3,00**
NIPUA-C_6-650-*5030*	5030	9.22 ± 2.46	10.2 ± 1.82	520 ± 51	17	0.89
NIPUA-C_6-2000/BD-1/2	2800	6.80 ± 0.58	9.17 ± 1.81	300 ± 37	18	1.61

[1] Average molecular weight between two acrylate functions.

[2] E = Young modulus; σ_r = breaking stress; ε_r = elongation at break.

[3] %HS = Hard segment percentage.

[4] Double bond concentration of the A-Ol oligomer.

* Very fragile material. Value of the best test.

** Estimated through the theoretical functionality of the A-C6-650/TMP-1/0.5 precursor (f = 2,33 and M_n= 1750 g/mol).

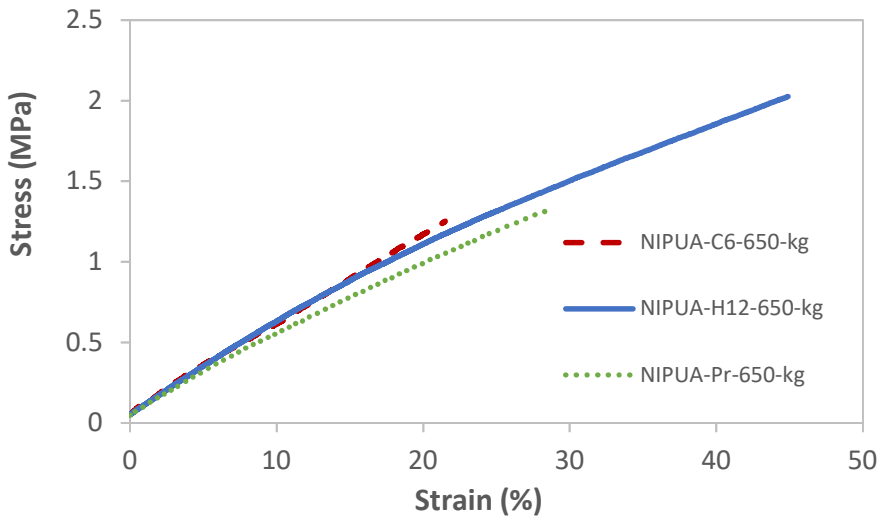

Figure 7: Typical stress/strain curves of the NIPUA-BMC-650 series.

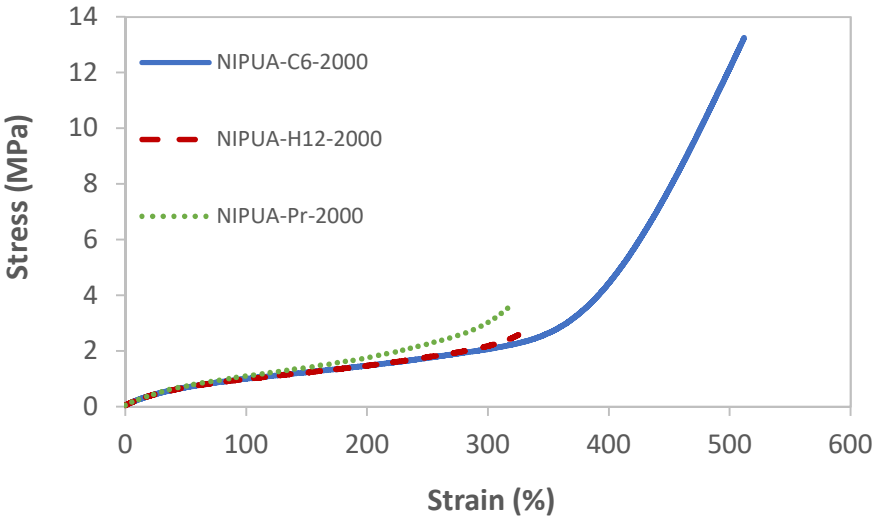

Figure 8: Typical stress/strain curves of the NIPUA-BMC-2000 series.

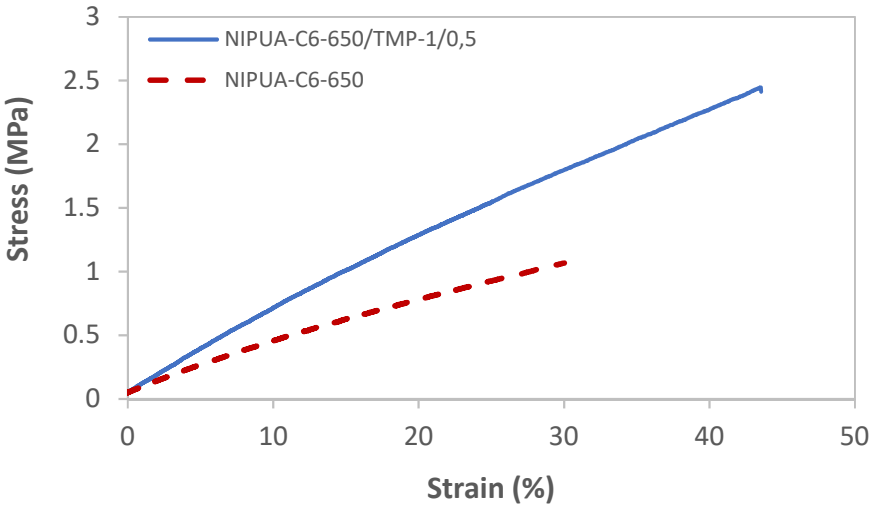

Figure 9: Typical stress/strain curves of NIPUA with and without TMP.

For the same molecular weight, the incorporation of trimethylolpropane (TMP) into the NIPUA structures improves all the mechanical parameters of the photo-crosslinked films (Figure 9 and Table 5). Indeed, its use has a double effect: - the percentage of urethane (%HS) is doubled, resulting in an increase in -H bonds; - the crosslinking density increases due to its trifunctional nature.

The impact of the increase in %HS can also be seen by comparing the properties between NIPUA-C6-2000-kg (%HS = 4.4%, Mc= 5650 g/mol) and NIPUA-C6-650-*5030* (%HS = 17%, Mc=5030 g/mol) coatings (Table 5, Figure 10). Stiffness properties are increased fourfold, i.e. E increased from 2.69 MPa to 9.22 MPa. However, strength properties (σ_r around 10.5 MPa) and elasticity (ε_r around 500 %) were quite similar.

NIPUA based on BD as the chain extender, exhibited Young's modulus E around 7 MPa, elongations at break ε_r around 300% and σ_r around 9 MPa (Figure 10, Table 5). Compared to NIPUA-C_6-2000-kg, NIPUA-C_6-2000/BD-1/2 exhibited higher percentage of hard segments (%HS), which

explain its higher rigidity, and exhibited lower molecular weight between knots ($M_{c(A\text{-}A)}$), which explain its lower elasticity. Nevertheless, these two parameters do not appear to have any influence on the ultimate stress at break.

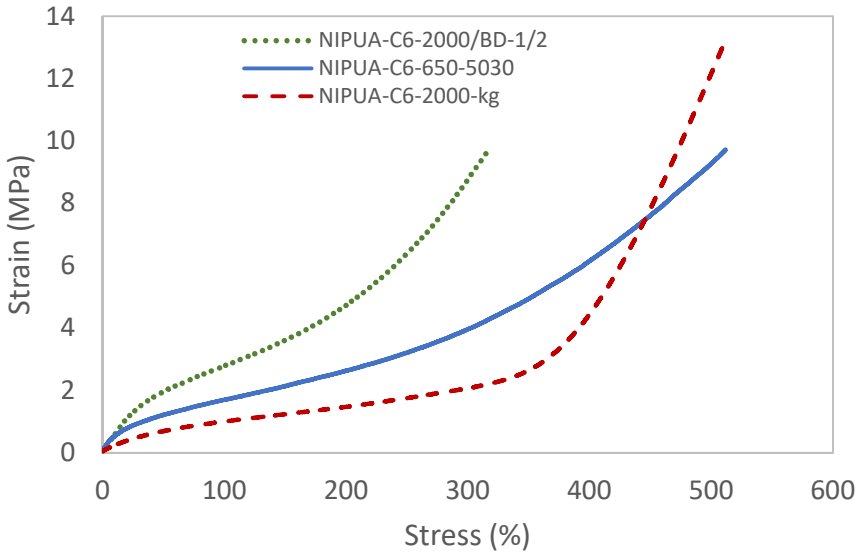

Figure 10: Typical stress/strain curves of NIPUA coatings with different urethane contents.

In summary, the incorporation of urethane functions effectively improves the mechanical properties of NIPUAs coatings, whether through the incorporation of a chain extender (BD) or a crosslinking agent (TMP), or by increasing the amount of urethane groups within the polymer backbone. However, the average molecular weight between knots must be sufficient to afford the elasticity properties.

CONCLUSIONS

NIPUs oligomers with exclusively acrylate chain-ends (A-OI) and controlled molecular weights were synthesized by transurethane polycondensation followed by reaction with acryloyl chloride. Ten NIPUs-acrylate coatings (NIPUAs) were prepared by photo-crosslinking of A-OI formulations under a high-intensity UV system. Analysis of the thermal and mechanical properties of NIPUAs coatings highlighted the importance of the urethane function, especially for increasing strength and rigidity of the materials, without excessive loss of elasticity. Thus, we have successfully synthesized a range of coatings with thermal and mechanical properties in line with those of the flexible PUs currently developed on the market, which can be amorphous or semi-crystalline ($T_{5\%}$ > 255°C, E = 2.6 – 9.2 MPa, σ_r up to 11.8 MPa, ε_r = 20 - 520 %) by a route that totally eliminates the use of isocyanates. Finally, some of the NIPUAs developed, in particular those based on the monomer BMC-C6, have biosourced carbon levels very close to 100%, where only the acrylate functions at the chain-ends derive from petroleum resources.

ACKNOWLEDGEMENTS

Authors thank Mäder research company for the financial support. ***This manuscript is a tribute to the 50 year anniversary of the French Polymer Group (Groupe Français des Polymères - GFP).***

Data availability

The processed data required to reproduce these findings are available to download from http://dx.doi.org/10.17632/7dnbdptv46.3.

REFERENCES AND NOTES

(1) J. Fu, L. Wang, H. Yu, M. Haroon, F. Haq, W. Shi, B. Wu, L. Wang, Research progress of UV-curable polyurethane acrylate-based hardening coatings, Prog. Org. Coatings. 131 (2019) 82–99. https://doi.org/10.1016/j.porgcoat.2019.01.061.

(2) S. Oprea, S. Vlad, A. Stanciu, Poly(urethane-methacrylate)s. Synthesis and characterization, Polymer 42 (2001) 7257–7266. https://doi.org/10.1016/S0032-3861(01)00206-3.

(3) S.D. Maurya, S.K. Kurmvanshi, S. Mohanty, S.K. Nayak, A Review on Acrylate-Terminated Urethane Oligomers and Polymers: Synthesis and Applications, Polym. - Plast. Technol. Eng. 57 (2018) 625–656. https://doi.org/10.1080/03602559.2017.1332764.

(4) H.J. Assumption, L.J. Mathias, Photopolymerization of urethane dimethacrylates synthesized via a non-isocyanate route, Polymer 44 (2003) 5131–5136. https://doi.org/10.1016/S0032-3861(03)00530-5.

(5) O.L. Figovsky, L. Shapovalov, R. Potashnikov, Z. Yury, B. J, D. Letnik, A. Schijuer, L. Shapovalov, R. Potashnikov, Y. Tzaid, J. Bordado, A. Schijuer, D. Letnik, Foamable photo-polymerized composition, US2004176485A1, 2004.

(6) Y. Huang, L. Pang, H. Wang, R. Zhong, Z. Zeng, J. Yang, Synthesis and properties of UV-curable tung oil based resins via modification of Diels-Alder reaction, nonisocyanate polyurethane and acrylates, Prog. Org. Coatings. 76 (2013) 654–661. https://doi.org/10.1016/j.porgcoat.2012.12.005.

(7) J.Z. Hwang, G.-J. Chang, J.-J. Lin, C.-W. Tsai, S.-C. Wang, P.-C. Chen, K.N. Chen, J.T. Yeh, Functional polyurethane prepolymer, method of preparing polyurethane by using the same, and application method thereof, US2013004677A1, 2013.

(8) G. Monnier, C. Leroy, Oligomères uréthane acrylates mono ou multifonctionnels sans isocyanate, WO 2016059340A1, 2016.

(9) G. Monnier, C. Duquenne, Oligomère uréthane acrylé ou méthacrylé sans isocyanate, WO 2014188116A1, 2014.

(10) J.Z. Hwang, S.C. Wang, P.C. Chen, C.Y. Huang, J.T. Yeh, K.N. Chen, A new UV-curable PU resin obtained through a nonisocyanate process and used as a hydrophilic textile treatment,

J. Polym. Res. 19 (2012). https://doi.org/10.1007/s10965-012-9900-y.

(11) X. Wang, M.D. Soucek, Investigation of non-isocyanate urethane dimethacrylate reactive diluents for UV-curable polyurethane coatings, Prog. Org. Coatings. 76 (2013) 1057–1067. https://doi.org/10.1016/j.porgcoat.2013.03.001.

(12) M.D. Soucek, L. Meng, Preparation of non-isocyanate urethane (meth)acrylates for urethane functional latex, US2016280807A1, 2016.

(13) O.L. Figovsky, L. Shapovalov, R. Potashnikov, Y. Tzaid, J. Bordado, A. Schijuer, D. Letnik, Foamable photo-polymerized composition, US2004176485A1, 2004.

(14) F. Zareanshahraki, H.R. Asemani, J. Skuza, V. Mannari, Synthesis of non-isocyanate polyurethanes and their application in radiation-curable aerospace coatings, Prog. Org. Coatings. 138 (2020) 105394. https://doi.org/10.1016/j.porgcoat.2019.105394.

(15) M. Unverferth, O. Kreye, A. Prohammer, M.A.R. Meier, Renewable non-isocyanate based thermoplastic polyurethanes via polycondensation of dimethyl carbamate monomers with diols, Macromol. Rapid Commun. 34 (2013) 1569–1574. https://doi.org/10.1002/marc.201300503.

(16) C. Duval, N. Kébir, A. Charvet, A. Martin, F. Burel, Synthesis and properties of renewable nonisocyanate polyurethanes (NIPUs) from dimethylcarbonate, J. Polym. Sci. Part A Polym. Chem. 53 (2015) 1351–1359. https://doi.org/10.1002/pola.27568.

(17) A. Martin, L. Lecamp, H. Labib, F. Aloui, N. Kébir, F. Burel, Synthesis and properties of allyl terminated renewable non-isocyanate polyurethanes (NIPUs) and polyureas (NIPUreas) and study of their photo-crosslinking, Eur. Polym. J. 84 (2016) 828–836. https://doi.org/10.1016/j.eurpolymj.2016.06.008.

(18) N. Kébir, S. Nouigues, P. Moranne, F. Burel, Nonisocyanate thermoplastic polyurethane elastomers based on poly(ethylene glycol) prepared through the transurethanization approach, J. Appl. Polym. Sci. 134 (2017) 1–9. https://doi.org/10.1002/app.44991.

(19) S. Li, Z. Sang, J. Zhao, Z. Zhang, J. Cheng, J. Zhang, Synthesis and properties of non-isocyanate aliphatic crystallizable thermoplastic poly(ether urethane) elastomers, Eur. Polym. J. 84 (2016) 784–798. https://doi.org/10.1016/j.eurpolymj.2016.08.007.

(20) Z. Shen, L. Zheng, C. Li, G. Liu, Y. Xiao, S. Wu, J. Liu, B. Zhang. A comparison of non-isocyanate and HDI-based poly(ether urethane): Structure and properties. Polymer 175 (2019) 186-194. https://doi.org/10.1016/j.polymer.2019.05.010.

(21) S. Li, J. Zhao, Z. Zhang, J. Zhang, W. Yang, Synthesis and characterization of aliphatic thermoplastic poly(ether urethane) elastomers through a non-isocyanate route, Polymer 57 (2015) 164-172. https://doi.org/10.1016/j.polymer.2014.12.009.

(22) A. Cornille, R. Auvergne, O. Figovsky, B. Boutevin, S. Caillol. A perspective approach to sustainable routes for non-isocyanate polyurethanes. Eur. Polym. J. 84 (2016) 828–836. https://doi.org/10.1016/j.eurpolymj.2016.11.027.

(23) R. H. Lambeth, T. J. Henderson, Organocatalytic synthesis of (poly)hydroxyurethanes from cyclic carbonates and amines, Polymer 54 (2013) 5568-5573. https://doi.org/10.1016/j.polymer.2013.08.053.

(24) C. Duval, N. Kébir, R. Jauseau, F. Burel, Organocatalytic synthesis of novel renewable non-isocyanate polyhydroxyurethanes, J. Polym. Sci. Part A Polym. Chem. 54 (2016) 758–764. https://doi.org/10.1002/pola.27908.

(25) P. F. H. Harmsen, M. M. Hackmann, H. L. Bos, *Biofuels, Bioprod. Biorefin.* **2014**, *8*, 306-324.

(26) R. Archer, G. M. Diamond, E. L. Dias, V. J. Murphy, M. Petro, J. D. Super, WO patent 2013090031 A2 20130620, **2013**.

(27) J.-C. Choi, L.-N. He, H. Yasuda, T. Sakakura, Selective and high yield synthesis of dimethyl carbonate directly from carbon dioxide and methanol, Green Chem. 4 (2002) 230–234. https://doi.org/10.1039/b200623p.

(28) R. Ballini, D. Fiorini, R. Maggi, P. Righ, G. Sartori, R. Sartori, TBD-catalysed solventless synthesis of symmetrically N,N'-substituted ureas from primary amines and diethyl carbonate, Green Chem. 5 (2003) 396-398. https://doi.org/10.1039/B301951A.

(29) Y. Suryawanshi, P. Sanap, V. Wani, Advances in the synthesis of non-isocyanate polyurethanes, Polym. Bull. 76 (2019) 3233–3246. https://doi.org/10.1007/s00289-018-2531-7.

(30) Cowie, J. M. G. *Polymers: Chemistry & Physics of Modern Materials (2nd edition)*; **1991**.

(31) Allcock, H. R.; Lampe, F. W.; Mark, J. E. *Contemporary Polymer Chemistry 3rd edition*; **2003**.

(32) O. Llorente, M.J. Fernández-Berridi, A. González, L. Irusta, Study of the crosslinking process of waterborne UV curable polyurethane acrylates, Prog. Org. Coatings. 99 (2016) 437–442. https://doi.org/10.1016/j.porgcoat.2016.06.020.

(33) H.D. Hwang, H.J. Kim, Enhanced thermal and surface properties of waterborne UV-curable polycarbonate-based polyurethane (meth)acrylate dispersion by incorporation of polydimethylsiloxane, React. Funct. Polym. 71 (2011) 655–665. https://doi.org/10.1016/j.reactfunctpolym.2011.03.004.

(34) S. Das, D.F. Cox, G.L. Wilkes, D.B. Klinedinst, I. Yilgor, E. Yilgor, F.L. Beyer, Effect of symmetry and H-bond strength of hard segments on the structure-property relationships of segmented, nonchain extended polyurethanes and polyureas, J. Macromol. Sci. Part B Phys.

46 (2007) 853–875. https://doi.org/10.1080/00222340701388805.

(35) M. Koshiba, K.K.S. Hwang, S.K. Foley, D.J. Yarusso, S.L. Cooper, Properties of ultra-violet curable polyurethane acrylates, J. Mater. Sci. 17 (1982) 1447–1458. https://doi.org/10.1007/BF00752259.

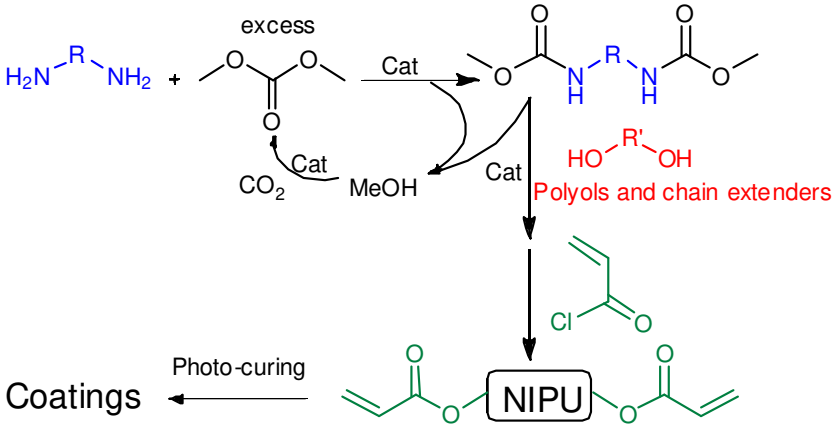
excess
Cat
Cat
CO2
MeOH
Cat
Polyols and chain extenders
Cl
Photo-curing
Coatings
NIPU